HYPERSPECTRAL REMOTE SENSING FOR SEASONAL ESTIMATION OF ABOVEGROUND BIOMASS IN GRASSLAND HABITATS

A. Psomas[a,b,*], M. Kneubühler[b], K. Itten[b], N. E. Zimmermann[a]

[a] Swiss Federal Research Institute WSL, Zuercherstrasse 111, 8903 Birmensdorf, Switzerland –
(achilleas.psomas, nez)@wsl.ch;
[b] Remote Sensing Laboratories (RSL), Dept. of Geography, University of Zürich, Winterthurerstrasse 190, 8057 Zürich,
Switzerland – (kneub, iiten)@geo.unizh.ch

Working Group VII/1 - Fundamental Physics and Modelling

ABSTRACT:

Dry grassland sites are amongst the most species rich habitats of Central Europe. In Switzerland, they are home to a large number of plant and animal species that are classified as endangered or threatened. A key component for designing optimal and effective management schemes ensuring the sustainability of these ecosystems, is knowledge of their biomass production. In this study we explored the potential of hyperspectral remote sensing for mapping above-ground biomass in grassland habitats along a dry-mesic gradient, independent of a specific habitat or a phenological period. We developed statistical models between spectral reflectance collected with a spectrometer but resampled to Hyperion bands, and biomass samples. We then tested to what degree the calibrated biomass models could be scaled to actual Hyperion data collected over the study area. Biomass samples (n = 155) were collected from 11 grassland fields located in the Central part of the Swiss Plateu. To capture normally occurring variation due to canopy growth stage and management factors sampling was performed at 4 time steps during the 2005 growing season. We investigated the relationship between biomass and a.) existing broad and narrow-band vegetation indices, b) narrow band NDVI type indices and c.) multiple linear regression using branch-and-bound variable search algorithms. Best models for estimating and predicting biomass were obtained from the multiple regression and narrow band NDVI type indices contrary to existing vegetation indices. Spectral regions related to plant water content were identified as the best estimators of biomass. Furthermore, results from this study demonstrated the importance of seasonal biomass measurements for building reliable models. Finally, promising results in estimating grassland biomass were not only obtained for the Hyperion resampled field spectrometer data, but also for the actual Hyperion data, showing the potential of up-scaling to the landscape level.

1. INTRODUCTION

Dry grassland sites are amongst the most species rich habitats of Central Europe. They originate from centuries of traditional land use and are a characteristic component of the cultural landscape in Europe. In Switzerland, conservation of biodiversity in these habitats is of major ecological importance. Almost 40% of plant and more than 50% of animal species living in these habitats are classified as endangered and are included in red lists (Eggenberg, 2001). Productivity and biomass of these grasslands have strong effects on both species competition and human management schemes, as higher productivity grasslands are more prone to be converted to agricultural areas. Therefore, development of robust and timely biomass estimates is of critical importance for monitoring and designing effective management practices that optimize sustainability of these ecosystems.

Direct measurements of grassland biomass are time consuming and expensive since they require extensive field work. In particular estimation of the spatial and temporal distribution of biomass at the landscape level is difficult to obtain from traditional methods. One of the major sources of information for the study of landscape and for estimating biomass over large areas is remote sensing (Kumar et al., 2001; Wylie, 2002). Attempts to estimate biomass using broadband sensors with spatial resolutions of 30m to 1km have resulted in a wide range of accuracies and precision (Dengsheng, 2006). In most of these

studies, quantity and variability of grassland biomass was estimated with vegetation indices calculated using the red and near-infrared bands of the broadband sensors.

Recently, new remote sensing instruments such as hyperspectral sensors (Van de Meer et al., 2001) that record many individual bands at very high spectral resolution have been developed. Studies using hyperspectral data to retrieve biomass have been carried out under controlled laboratory conditions (Filella, 2004; Mutanga, 2004) or in the field for vegetation types like wheat or corn that show low spatial variability of biomass (Hansen, 2003; Osborne et al., 2002; Xavier et al., 2006). Few studies only exist that have investigated the relationship between hyperspectral remote sensing and biomass production of mixed grassland ecosystems (He, 2006; Mirik et al., 2005; Tarr et al., 2005) and none, to our knowledge, that has extended such analyses over a growing season.

The objective of our study was to develop a method using field spectrometer data for estimating above ground biomass in grassland habitats along a dry-mesic gradient. The method should be independent of specific habitats or phenological period. We further investigated to what degree the calibrated biomass estimation could be scaled to Hyperion hyperspectral data. By this, we aimed at evaluating the potential to scale models calibrated from plot based estimates to larger landscapes as seen from spaceborne sensors.

2. MATERIALS AND METHODS

2.1 Study area

The study was conducted on the Central part of the Swiss Plateu around 8°02' E, 47°25'N near the village of Küttingen. The elevation of the area ranged from 350 to 500 m. Four characteristic grassland types were sampled (Table.1) that were previously mapped in a national mapping campaign (Eggenberg, 2001). The four semi-natural grassland types (AE, AEMB, MBAE, MB) were selected according to their position along a wet-dry gradient. AE is a species-rich Arrhenatherion type managed grassland, that is mesic and nutrient rich. The mesic and species-rich type AEMB includes tall, dense and multi-layered stands composed of many grasses, several herb species, and is still comparably nutrient-rich . In this type, canopy layers close to the ground are relatively damp and cool as a result of the dense growth. The type MBAE stands in-between AEMB and MB with respect of species richness, nutrients and canopy height. Finally, true semi-dry MB grasslands are comparably nutrient-poor and are generally dominated by *Bromus erectus* or *Brachypodium pinnatum* with stems standing well above the surrounding shorter herb vegetation. These stands are generally colourful and rich in herbs and species in general. The main management practice of the grasslands in the study area is for production of hay and only a few are used as pastures.

Type code	Phytosociology	Description
AE	species-rich Arrhenatherion type	Mesic, species rich, nutrient–rich, managed
AEMB	Transition Arrhenatherion to Mesobromion	Moderately-mesic, species-rich
MBAE	Transition Mesobromion to Arrhenatherion	Moderately-dry, species-rich
MB	Mesobromion type	Species-rich, semi-dry grassland

Table 1. Description of the four grassland types sampled

2.2 Biomass sampling

A total of 11 fields belonging to the 4 grassland types were selected from the existing national campaign map. The fields were chosen to have a total area larger than 5 Hyperion pixels and were checked for purity: we only kept grasslands, where the major vegetation type covered at least 75% of the mapped polygon. Sampling was performed at four times during the growing season of 2005 (10th June, 23rd June, 28th July, 10th August). We did so to ensure that normally occurring variation due to canopy growth stage and management factors was included in the dataset and the subsequent statistical models. Biomass samples were clipped at ground level using a 32cm radius metal frame. Within each field, 3 randomly selected plots were sampled to account for the spatial variability of the grassland habitats and to assist with the up-scaling of the analysis to the landscape-Hyperion level. A total of 155 biomass samples were collected. The collected material was stored in pre-weighted air-sealed plastic bags and transferred to the laboratory where the total fresh biomass was measured. Then samples were dried in the oven at 65 ^{o}C for 72h and weighted again to measure the water content and total dry biomass.

2.3 Field-Satellite Spectral Measurements

Spectral profiles of the grassland types were collected using the Analytical Spectral Devices (ASD) FieldSpec Pro FR spectrometer. This spectrometer has a 350-2500 nm spectral range and 1 nm spectral resolution with a 25° field-of-view. Collected spectra were converted to absolute reflectance by reference measurements over a Spectralon reflectance panel (Labsphere, Inc., North Sutton, N.H.) with known spectral properties. Calibration of the spectrometer was made every 20 measurements to minimize changes in atmospheric condition. Measurements were collected under sunny and cloud free conditions between 10:00 and 16:00 h while walking along 2 diagonal transects across the length of every field. This resulted in 60-100 spectral measurements per field, which ensured that the sampling would cover the spectral variability within each field. Measurements were taken from nadir at a height of ~1.5m above vegetation canopy. Field spectra were then resampled to simulate Hyperion spectral bands. Finally, after removal of erroneous measurements, the mean spectral reflectance of each grassland field was calculated.

Hyperion Level 1R data were acquired over the study area at nadir (overhead) pass on August 10, 2005 at 10:06:49 GMT. The EO-1 satellite has a sun-synchronous orbit at 705 km altitude. Hyperion collects 256 pixels with a size of 30 m on the ground over a 7.65 km swath. Data is acquired in pushbroom mode with two spectrometers. One operates in the VNIR range (70 bands between 356-1058 nm with an average FWHM of 10.90 nm) and the other in the SWIR range (172 bands between 852-2577 nm, with an average FWHM of 10.14 nm). From the 242 Level 1R bands, 44 are set to zero by software (bands 1-7, 58-76, 225-242). Post-Level 1R data processing of the acquired Hyperion scene included correction for striping pixels, smoothing using forward and inverse Minimum Noise Fraction transformation (MNF) (Datt et al., 2003), atmospheric correction using ATCOR-4 (Richter, 2003) and georectification of the scene using 25 ground control points. After removal of Hyperion bands that: were set to zero, were weak and with noisy signal and were strongly affected by atmospheric water, a total of 167 bands were available for further analysis (426 – 2355 nm).

2.4 Statistical analyses

The mean spectral reflectance of the 60-100 spectral measurements and the mean biomass of the 3 samples collected at each grassland field were used in the statistical analysis. Initial analysis revealed a heavily skewed distribution of the biomass data. In order to improve the regression modelling we log-transformed the biomass data so they would approach a normal distribution. Statistical models were calibrated with field spectrometer reflectance data resampled to simulate Hyperion bands.

Firstly we evaluated the relationship between biomass and normalised differences indices (NDVI, SR, RDVI, TVI), red edge indices (GMI, CI, VOG$_a$, RESP), three band indices (MCARI, TRVI, MCARI1) and soil line indices (SAVI, MSAVI, SARVI). A detailed description about properties and advantages of these indices can be found in Broge and Leblanc (2000) and in Haboudane et al. (2004).

However, most of the above mentioned indices consider only certain parts of the spectrum, primarily the chlorophyll absorption region (680nm), the NIR reflectance (800nm) and

the green reflectance peak (550nm). Given this limitation and in an attempt to make use of the large number of narrow bands of hyperspectral data we built narrow band NDVI-type (nb_NDVI$_{type}$) indices as shown in Eq. (1).

$$nb\_NDVI_{type}[\lambda_1, \lambda_2] = \frac{\lambda_1 - \lambda_2}{\lambda_1 + \lambda_2} \qquad (1)$$

All possible two-pair combinations were used in Eq. (1) where λ_1 and λ_2 were the Hyperion simulated bands from the field reflectance measurements. A total of 27,889 narrow band indices were calculated. These indices were used in linear regression models to determine their relationship with measured biomass.

The disadvantage of existing indices and of the nb_NDVI$_{type}$ indices is that they only consider a few of the available hyperspectral bands. Even though much of the information provided by neighbouring bands is often redundant (Thenkabail, 2004) it is still possible that the spectral information is not optimally used by these indices. Therefore, multiple linear regression (MLR) that selects the best combination of linear predictors from the Hyperion simulated bands was used for biomass estimation along the growing season. Branch-and-bound (b&b) (Miller, 2002) variable search algorithms were used to find spectral bands that best explained biomass.

The overall capability of each model in explaining the variability in the biomass was evaluated by the adjusted coefficient of determination (adj.R^2). We used the adj.R^2 since it will only increase if the new variable added will improve the model more than would be expected by chance. The model prediction error for estimating biomass was assessed by using a cross-validation (CV) procedure (Diaconis and Efron, 1983). With CV predicted samples are not used to build the model, so the Root Mean Square Error (RMSE) calculated is a good indicator of the model accuracy and predictive power. Cross-validation RMSE (CV-RMSE) was estimated by using all the biomass samples collected during the growing season. Nevertheless, to investigate the effect of seasonal variability we used a 4-fold "Date" CV procedure. By this, we calibrated models using data collected from three dates and then validated their predictions with data collected on the fourth. This process was repeated 4 times until each date was used for validation of model predictions once. Finally, the models with the highest accuracy and predictive power were used on the geometrically and atmospherically corrected Hyperion scene to predict the spatial distribution of biomass over the study area.

3. RESULTS AND DISCUSSION

Before the analysis of the relationship between biomass and remotely sensed data, descriptive biomass statistics were generated and are presented in Table 2 and Figure 1. Highest variability of biomass measurements was observed on the first (10th June) and second (23rd June) sampling dates. This happened since the grasslands sampled were along a dry-mesic gradient having different availability to water and nutrients and eventually different rates of growth and biomass accumulation. Lower biomass variability observed later on the season could be partly attributed to the management practices (cutting) applied on these fields.

Models using existing indices (e.g., NDVI, SAVI, MCARI, VOG$_a$) gave poor adj. R^2 values (Table 3). Marginally better results were obtained for SAVI. This index corrects for the soil background reflectance thus improving the model since many grassland fields did not have complete canopy cover during the season. Models for estimating biomass that used recently developed narrow band indices (e.g., MCARI, TVI, VOG$_a$) did not produce higher adj.R^2 (not all results shown here).

		Biomass (kg/m^2)				
	n	Mean	stdev	Min	Max	Range
Original	50	0.7756	0.5704	0.1785	3.3180	3.1395
Log-transf.	50	-0.4523	0.6186	-1.7230	1.1990	2.9220

Table 2. Summary statistics for original and log-transformed measured biomass at 50 grassland fields over 4 time steps during the 2005 growing season

All possible two band combinations were used to create nb_NDVI$_{type}$ indices. Regression coefficients (adj.R^2) between biomass and each nb_NDVI$_{type}$ index were determined and graphically presented in Figure 3. The adj.R^2 values ranged from 0.007 to 0.72 reflecting a wide variation in the strength of the relationship between nb_NDVI$_{type}$ indices and biomass. Compared to existing indices that primarily use the red and NIR parts of the spectrum, our analysis identified regions from the far-NIR and SWIR resulting in much higher adj.R^2 values (Table 3). High adj.R^2 values were found clustered in three spectral regions, namely: 1230nm, 1680nm and 2280nm. These parts of the spectrum are strongly related to plant leaf water content that has a correlation to canopy biomass and LAI (Hunt, 1991) and to cellulose, starch, lignin and nitrogen concentrations (Kumar et al., 2001). Our results, and in particular the nb_NDVI$_{type}$ indices formed from bands around 1700 and 1170 nm confirm findings of earlier studies (Cook et al., 1989; Hunt, 1991) that correlate the ratio between NIR and SWIR to productivity and LAI. The use of nb_NDVI$_{type}$ indices for estimating biomass did not only improve the adj.R^2, but also reduced the CV-RMSE thus the overall prediction accuracy of the models.
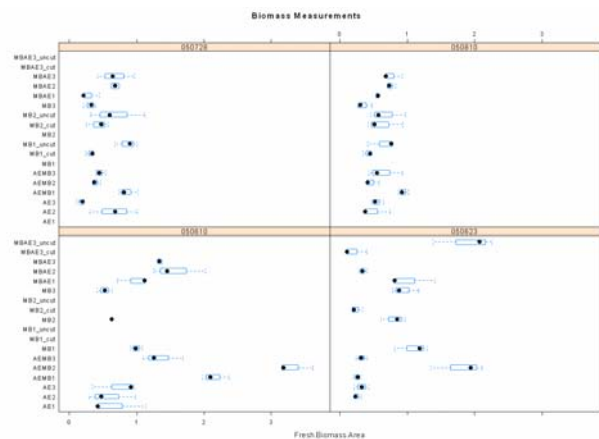
Figure 1. Mean biomass measurements of individual sampled fields during the growing season

Results of the multiple regression models for estimating biomass from spectral reflectance are listed in Table 3. We only built models using up to 4 spectral bands, since accuracies improved only marginally above this number and because we had too few measurements to build models with a high number

of predictors. Although selection of spectral bands was solely based on statistical optimisation of the models, these bands were located at key spectral regions with respect to physical processes of vegetation. The 472, 522 nm bands from the visible region can be correlated with chlorophyll content of vegetation, the 1202 nm from the NIR and the 1716 nm from the SWIR are related to plant leaf water content (Hunt, 1991) and the 2266 nm region to biochemical canopy properties like cellulose, starch and lignin (Elvidge, 1990). Even though models used slightly different bands, these were neighbouring and highly correlated to the ones mentioned above and thus provided the same type of information.

Model	Adj.R2	CV-RMSE
SAVI	0.29	0.53
NDVI	0.28	0.51
VOG$_a$	0.22	0.54
nb_NDVI$_{type}$ b1715,b1172	0.61	0.39
nb_NDVI$_{type}$ b1092,b2266	0.52	0.43
MLR-2 bands b482,b1785	0.77	0.29
MLR-2 bands b472,b1785	0.77	0.31
MLR-3 bands b522,b1695,b1715	0.82	0.27
MLR-3 bands b1192,b1202,b1232	0.82	0.29
MLR-4 bands b522,b1212,b1232,b1715	0.86	0.23
MLR-4 bands b522,b1212,b1232,b1705	0.86	0.25

Table 3. Adjusted regression coefficient (adj.R^2) and prediction error (CV-RMSE) of the best models for the three approaches (existing indices, nb_NDVI$_{type}$ indices, MLR) for estimating grassland biomass
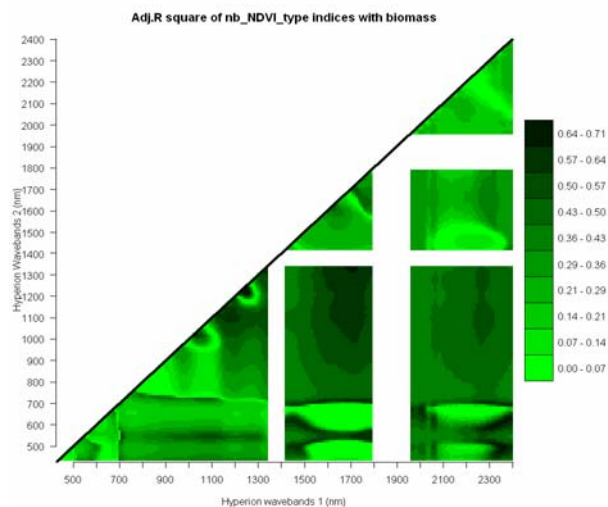
Figure 2. Result of the nb_NDVI$_{type}$ indices analyses. The graph shows the correlations (adj.R^2) between biomass and nb_NDVI$_{type}$ indices calculated from any band pairs among the simulated Hyperion bands. Darker areas indicate higher adj.R^2. White gaps are strong water absorption regions that were removed from the analysis

An overall comparison of the strength of the model fit and prediction errors is presented in Figure 4 and 5. Models that used existing indices developed either for broadband or hyperspectral sensors showed comparably poor performance with adj.R^2 ranging from ~0.21 to ~0.29. Development of new nb_NDVI$_{type}$ indices greatly improved the adj.R^2 from 0.29 to 0.61. Relatively similar increase was observed when 2-band MLR models were used for biomass estimation since model

adj.R^2 improved from 0.61 to 0.77. Incorporation of more bands in the MLR models further increased the adj.R^2 moderately (0.7783 for 3-band MLR and 0.8631 for 4-band MLR). Model prediction errors followed a similar pattern. In particular, models using existing indices showed high CV-RMSE (0.5323) that gradually reduced when nb_NDVI$_{type}$ (0.3961) and MLR (0.2935 to 0.2357) models were used for biomass estimation.

Calibration-Validation dates	RMSE				
	Exist. indices	nb_ NDVI$_{type}$	2-band MLR	3-band MLR	4-band MLR
C-2,3,4/V-1	0.67	0.49	0.40	0.34	0.30
C-1,3,4/V-2	0.65	0.50	0.36	0.31	0.34
C-1,2,4/V-3	0.50	0.26	0.21	0.20	0.14
C-1,2,3/V-4	0.44	0.39	0.28	0.25	0.25
Mean-CV	0.56	0.41	0.31	0.27	0.25

Table 4. Prediction errors of best models build with the three approaches. Models were calibrated on three dates and validated on the fourth. C-2,3,4/V-1 means that regression models were calibrated on Dates 2,3,4 and validated on Date 1. Recording dates are, Date-1: 10th June, Date-2: 23rd June, Date-3: 28th July and Date-4: 10th August
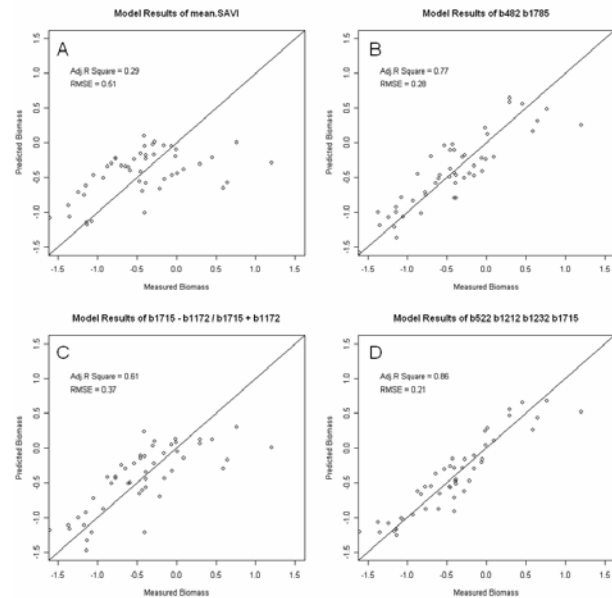
Figure 3. Best measured vs. predicted biomass estimates originating from regression models of A) existing indices, B) 2-band MLR, C) nb_NDVI$_{type}$, and D) 4-band MLR, optimized with a 4-fold cross-validation using samples from all four sampling dates

The best models of each of the three approaches (existing indices, nb_NDVI$_{type}$ indices, MLR) were used in the 4-fold "Date" CV analyses (Table 4). A clear pattern was observed. Models calibrated from biomass samples collected in the first two sampling dates of the season predicted biomass with lower RMSE. Contrary, models calibrated using samples from only one of these dates gave poorer predictions. For example, the best nb_NDVI$_{type}$ index model for estimating biomass when calibrated with samples from Date 1 and Date 2 yielded RMSE of 0.2669 and 0.3990 that increased to 0.4905 and 0.5022 when samples from only one of these dates were used. This may reflect the high variability of biomass samples collected on Date 1 and Date 2 (Fig. 1). Models calibrated from data from

these dates could account for a much broader range of variability of biomass. Contrary, model calibration with samples from only one of these dates was not sufficient to explain the variability observed on the samples collected on the other date. Thus, when models had to predict these values they produced higher errors.
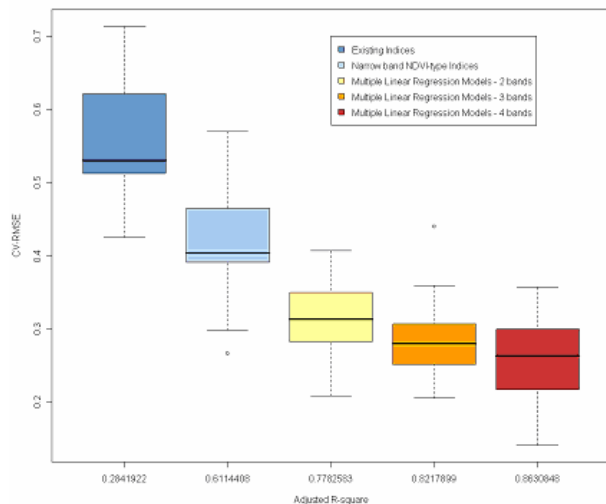
Figure 4. Boxplots of model calibration strength (adj.R^2) against prediction error (CV-RMSE) for the best three performing models of the three modelling approaches

Preliminary results of the spatial distribution of biomass over the study area, from up-scaling the statistical models to the Hyperion scene, are shown in Figure 6. This was done by applying the models calibrated with field spectrometer data resampled to simulate Hyperion bands, to the actual Hyperion scene acquired over the study area. Even thought models were calibrated for grassland habitats, forested areas could immediately be observed (dark areas) as high biomass was predicted for these habitats. High variation of predicted biomass values on grassland habitats (areas between dark forest patches) showed the sensitivity of the models in predicting subtle changes of in-field biomass variability. Validation of the model predictions (results not shown here) with field samples collected on the date of the Hyperion acquisition, gave similar prediction errors as obtained from the CV procedure. Cut grasslands with low biomass were correctly predicted and are shown with very light colours. However, over-estimation and higher errors were observed for areas adjacent to forests. This was due to the mixed pixels that affected the spectral signal recorded by the sensor and thus the model prediction.
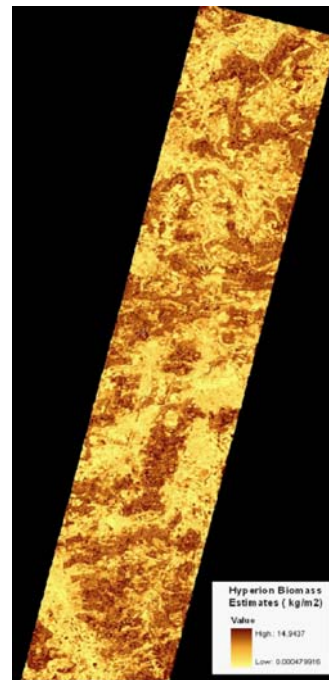
Figure 5. Biomass prediction map (Kg/m^2) created from Hyperion reflectance values, using the nb_NDVI$_{type}$ index regression model constructed with bands at b1715nm and b1172nm

4. CONCLUSIONS

Results presented in this paper showed the high potential of hyperspectral remote sensing for estimating biomass of grassland habitats along a dry-mesic gradient. Our analyses demonstrated the importance of acquiring biomass measurements along the growing season in order to capture the variability observed and eventually be able to create reliable and more accurate models. This is specifically important in managed grasslands since management activities introduce a high variability in phenological states. Furthermore, we illustrated the necessity of developing new indices since existing vegetation indices using information from the red and near-infrared regions yielded poor biomass estimation results. Rather, spectral regions related with plant leaf water content should be used as they appear to be more suitable for estimating and predicting biomass. Use of multiple linear regression always gave better models for estimation and prediction of biomass. In addition, branch-and-bound (b&b) variable search algorithms proved a powerful statistical approach since bands selected made sense with respect to physical processes of vegetation. Nevertheless, attention should be paid to the number of bands used in the multiple regression models since accuracy does not improve after a certain point and addition of extra bands will only reduce the quality of the models. Finally, preliminary results from up-scaling to Hyperion level showed that we could achieve high accuracies provided that multiple samples covering the in-field variability of biomass have been acquired.

REFERENCES

Broge, N.H. and Leblanc, E., 2000. Comparing prediction power and stability of broadband and hyperspectral vegetation indices for estimation of green leaf area index and canopy chlorophyll density. Remote Sensing of Environment, 76(2): 156-172.

Cook, E.A., Iverson, L.R. and Graham, R.L., 1989. Estimating forest productivity with Thematic Mapper and biogeographical data. Remote Sensing of Environment, 28: 131-141.

Datt, B., McVicar, T.R., Van Niel, T.G., Jupp, D.L.B. and Pearlman, J.S., 2003. Preprocessing EO-1 Hyperion Hyperspectral Data to Support the Application of Agricultural Indexes. IEEE TRANSACTIONS ON GEOSCIENCE AND REMOTE SENSING, 41(2): 1246-1259.

Dengsheng, L., 2006. The potential and challenge of remote sensing-based biomass estimation. International Journal Of Remote Sensing, 27(7-8): 1297-1328.

Diaconis, P. and Efron, B., 1983. Computer-intensive methods on statistics. Scientific American, 248: 96-108.

Eggenberg, S.D., Thomas; Dipner, Michael & Mayer, Cornelia, 2001. Cartography and evaluation of dry grasslands sites of national importance:Technical report.Environmental Series No. 325, published by Swiss Agency for the Environment, Forests and Landscape (SAEFL), Berne.

Elvidge, C.D., 1990. Visible and near infrared reflectance characteristics of dry plant materials. International Journal Of Remote Sensing, 11(10): 1775-1795.

Filella, I.P.u., Josep; Llorens, Laura & Estiarte, Marc, 2004. Reflectance assessment of seasonal and annual changes in biomass and CO2 uptake of a Mediterranean shrubland submitted to experimental warming and drought. Remote Sensing of Environment, 90(3): 308-318.

Haboudane, D., Miller, J.R., Pattey, E., Zarco-Tejada, P.J. and Strachan, I., 2004. Hyperspectral vegetation indices and novel algorithms for predicting green LAI of crop canopies: Modeling and validation in the context of precision agriculture. Remote Sensing of Environment, 90(3): 337-352.

Hansen, P.M.S., J. K., 2003. Reflectance measurement of canopy biomass and nitrogen status in wheat crops using normalized difference vegetation indices and partial least squares regression. Remote Sensing of Environment, 86(4): 542-553.

He, Y.G., Xulin & Wilmshurst, John, 2006. Studying mixed grassland ecosystems I:suitable hyperspectral vegetation indices. Canadian Journal of Remote Sensing, 32(2): 98-107.

Hunt, E.R., 1991. Airborne remote sensing of canopy water thickness scaled from leaf spectrometer data. International Journal Of Remote Sensing, 12(3): 643–649.

Kumar, L., Schmidt, K.S., Dury, S. and Skidmore, A.K., 2001. Imaging spectrometry and vegetation science. In: F.d.J. van de Meer, S.M (Editor), Imaging Spectrometry.Basic principles and prospective applications. Kluwer Academic Press, Dordrecht, pp. 111-155.

Miller, A.J., 2002. Subset selection in regression. Chapman & Hall/CRC, Boca Raton, Florida.

Mirik, M., Norland, J.E., Crabtree, R.L. and Biondini, M.E., 2005. Hyperspectral one-meter-resolution remote sensing in yellowstone national park, wyoming I. Forage nutritional values. Rangeland & ecology management, 58(5): 452-458.

Mutanga, O.S., Andrew K., 2004. Hyperspectral band depth analysis for a better estimation of grass biomass (Cenchrus ciliaris) measured under controlled laboratory conditions. International Journal of Applied Earth Observation and Geoinformation, 5(2): 87-96.

Osborne, S.L., Schepers, J.S., Francis, D.D. and Schlemmer, M.R., 2002. Use of Spectral Radiance to Estimate In-Season Biomass and Grain Yield in Nitrogen- and Water-Stressed Corn. Crop Science, 42(1-2): 165-175.

Richter, R., 2003. Atmospheric / Topographic Correction for Airborne Imagery. ATCOR-4 User Guide, Version 3.0,. DLR-IB564-02/03, DLR, pp.66., 66 pp.

Tarr, A.B., Moore, K.J. and Dixon, P.M., 2005. Spectral reflectance as a covariate for estimating pasture productivity and composition. Crop Science, 45(3): 996-1003.

Thenkabail, P.S.E., Eden A.; Ashton, Mark S. & Van Der Meer, Bauke, 2004. Accuracy assessments of hyperspectral waveband performance for vegetation analysis applications. Remote Sensing of Environment, 91(3-4): 354-376.

Van de Meer, F., de Jong, S.M. and Bakker, W., 2001. Imaging spectrometry for agriculture. In: F.d.J. van de Meer, S.M (Editor), Imaging Spectrometry.Basic principles and prospective applications. Kluwer Academic Press, Dordrecht, pp. 157-199.

Wylie, B.K.M., D.J.; Tieszen, L.L. & Mannel, S., 2002. Satellite mapping of surface biophysical parameters at the biome scale over the North American grasslands A case study. Remote Sensing of Environment, 79(2-3): 266-278.

Xavier, A.C. et al., 2006. Hyperspectral field reflectance measurements to estimate wheat grain yield and plant height. Scientia Agricola, 63(2): 130-138.